Low-complexity Noncoherent Iterative CPM Demodulator for FH Communication

Yonggang WANG, Aijun LIU, Daoxing GUO, Xian LIU

Institute of communication engineering, PLA University of Science and Technology,
Yudao Street, 2, 210007, Nanjing, China

wangyg1984@163.com, Ajliu1970@163.com, Dxguo1973@163.com, liux1981@126.com

Abstract. *In this paper, we investigate the noncoherent iterative demodulation of coded continuous phase modulation (CPM) in frequency hopped (FH) systems. In this field, one important problem is that the complexity of the optimal demodulator is prohibitive unless the number of symbols per hop duration is very small. To solve this problem, we propose a novel demodulator, which reduces the complexity by applying phase quantization and exploiting the phase rotational invariance property of CPM signals. As shown by computational complexity analysis and numerical results, the proposed demodulator approaches the performance of the optimal demodulator, and provides considerable performance improvement over the existing solutions with the same computational complexity.*

Keywords

Continuous phase modulation, frequency hopping, noncoherent demodulation, iterative demodulation, low-complexity.

1. Introduction

Frequency hopping (FH) is a widely used technique in wireless communication systems, e.g., military anti-jamming communication system and cognitive radio system. One characteristic of FH system is the phase discontinuity between adjacent hop intervals. Consequently, compared with coherent demodulation that requires additional overhead for channel estimation, noncoherent demodulation is more preferred in practical systems, since it does not require explicit knowledge or estimation of channel phase. Moreover, next generation FH communication requires a spectrum efficient transmission waveform that allows the use of low-cost power-efficient amplifiers. In this context, continuous phase modulation (CPM) [1] serves as a good candidate due to its high spectral efficiency and constant envelope property.

In this paper, we investigate the noncoherent iterative demodulation of coded CPM in FH systems. In this field, one important problem is that the complexity of the optimal demodulator is exponential to the hop length (i.e., the number of symbols per hop duration) and thus become prohibitive even for moderate hop length [2]. In order to reduce the complexity, several suboptimal demodulators have been proposed in previous literatures. In [2], a suboptimal demodulator is proposed based on multiple symbol differential detection (MSDD) [3], which evaluates soft symbol decisions over an observation window. However, the performance of the demodulator suffers significant losses as the window size is much smaller than the hop length, at the same time its complexity increases exponentially with the window size. Another suboptimal demodulator [4], [5] is proposed based on the iterative tree search (ITS) and employs M-algorithm [6] to limit the number of paths through the tree. However, the performance of the demodulator suffers significant losses due to two reasons, i.e., only part of the symbols over the hop duration is used to evaluate the soft symbol decisions and the correct path through the tree may be discarded by M-algorithm.

In this paper, a novel noncoherent iterative CPM demodulator for FH communication is proposed. We reduce the complexity by the following three steps. First, we introduce phase quantization [7] into noncoherent demodulation of CPM. In such way, the complexity of noncoherent demodulation is reduced to a level that is comparable to coherent receivers. Second, the phase invariance property of CPM signals [8] is exploited to further reduce the complexity of the proposed demodulator. Furthermore, the phase branch pruning approach [7] is integrated into the proposed demodulator to offer a good trade-off between the complexity and performance. We analyze the computational complexity of our proposed demodulator and evaluate its performance by numerical simulations. It is shown that the proposed demodulator approaches the performance of the optimal noncoherent demodulator, while its complexity grows linearly with the hop length. Moreover, compared with the demodulators presented in [2] and [4], [5], the proposed scheme achieves considerable performance improvement with the same computational complexity.

The rest of the paper is organized as follows. The system model is described in Section 2. The proposed low-complexity demodulator is derived in Section 3. Computational complexity analysis and numerical results are pre-

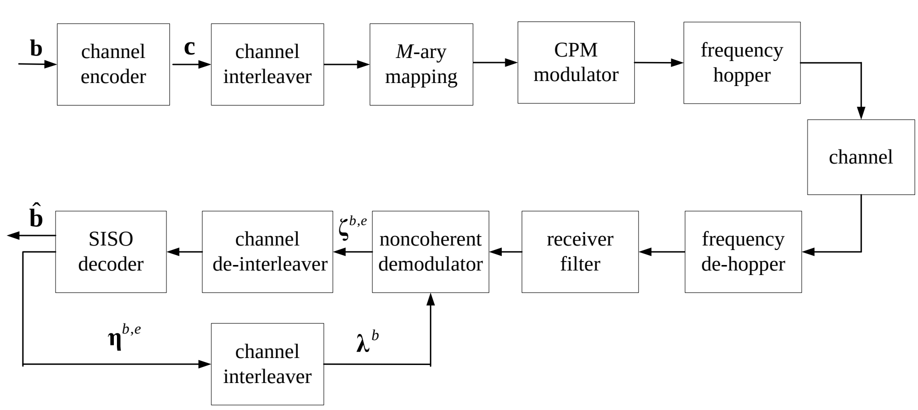

Fig. 1. Schematic block diagram of the system.

sented in Section 4 and Section 5, respectively. Finally, conclusions are drawn in Section 6.

2. System Model

2.1 Signal Model

The M-ary CPM signal in the interval $nT_s \le t \le (n+1)T_s$ is described as

$$s(t;\mathbf{a},\varphi_0,a_{-L+1},\cdots,a_{-1})=\sqrt{\frac{2E_s}{T_s}}\exp[j\varphi(t;\mathbf{a},\varphi_0,a_{-L+1},\cdots,a_{-1})] \quad (1)$$

with

$$\varphi(t;\mathbf{a},\varphi_0,a_{-L+1},\cdots,a_{-1})=\varphi_n+2\pi h\sum_{i=n-L+1}^{n}a_i q(t-iT_s) \quad (2)$$

and

$$\varphi_n=(\varphi_0+\pi h\sum_{i=-L+1}^{n-L}a_i) \bmod 2\pi \quad (3)$$

where E_s is the symbol energy, T_s is the symbol interval, and $\mathbf{a}$ is the input symbol sequence with i-th symbol $a_i \in \{\pm1,\pm3,\cdots,\pm M-1\}$. $h=Q/P$ is the modulation index, where Q and P are relative prime integer. The phase pulse $q(t)$ is the time-integral of a frequency pulse with length LT_s and area 1/2, where L is the length of phase pulse. Moreover, $\varphi_0 \in \{2\pi/P, 4\pi/P,\cdots,2\pi(P-1)/P\}$ and $a_{-L+1},\cdots,a_{-1} \in \{\pm1,\pm3,\cdots,\pm M-1\}$ denote the initial parameters for the CPM modulator.

According to the well known Rimoldi decomposition [9], the CPM modulator can be represented as a cascade of a continuous phase encoder (CPE) and a memoryless modulator. The CPE, in general, is a time-invariant convolutional encoder operating on a ring of integers modulo P. Therefore, by adding an outer convolutional encoder connected to the CPE through an interleaver, a serial concatenated convolutional encoder system [10], [11] is formed. Subsequently, iterative demodulation and decoding can be performed based on maximum a posteriori detection at the receiver.

2.2 Channel Model

Usually, at the baseband, the FH channel is modeled as an additive white Gaussian noise (AWGN) channel where the phase offset is assumed to remain constant over each hop and independent from one hop to the next [2]. After dehopped and filtered, the baseband received signal of the k-th hop is described as

$$r_k(t)=s_k(t;\mathbf{a}_k,\varphi_{0,k},a_{-L+1,k},\cdots,a_{-1,k})\exp(j\theta_k)+w(t) \quad (4)$$

over the interval $iT_s \le t \le (i+1)T_s$. Here, $k=\lfloor i/N \rfloor$, and the function $\lfloor x \rfloor$ rounds x down to an integer value. N is the number of symbols per hop and defined as hop length. The symbols of the k-th hop, i.e., $\{a_{kN},a_{kN+1},\cdots,a_{kN+N-1}\}$, are denoted as $\mathbf{a}_k=\{a_{0,k},a_{1,k},\cdots,a_{N-1,k}\}$, and the last $L-1$ symbols of the $(k-1)$-th hop, i.e., $a_{kN-L+1},\cdots,a_{kN-1}$, are denoted as $a_{-L+1,k},\cdots,a_{-1,k}$. The initial phase of the k-th hop, i.e., φ_{kN}, is denoted as $\varphi_{0,k}$. Moreover, $w(t)$ denotes the additive white Gaussian noise with power spectral density N_0 W/Hz, and θ_k represents the phase offset for the k-th hop. θ_k is uniformly distributed over the range $[0,2\pi)$, and is modeled as independent from one hop to the next.

2.3 System Description

Fig. 1 shows a schematic block diagram of the overall system. The channel encoder encodes a sequence of information bits $\mathbf{b}$ into a sequence of coded bits $\mathbf{c}$. The resulting coded sequence is interleaved by a random permutation and is then mapped to a sequence of M-ary symbols. The M-ary sequence is then passed to the CPM modulator, which acts as an inner recursive encoder. Subsequently, a frequency hopper hops the carrier over different frequencies.

At the receiver end, a frequency de-hopper drives the CPM signal back to base band. Subsequently, for each hop of received samples, the hop-wise demodulator computes a posteriori probabilities (APPs) ζ^s of the input CPM symbols. These symbol APPs are then used to compute bit-wise APPs ζ^b. The extrinsic part of these bit-wise APPs $\zeta^{b,e}$ are then de-interleaved and passed to the channel decoder. The channel decoder performs one decoding iteration and generates the bit-wise extrinsic information $\eta^{b,e}$. Then the interleaved bit-wise extrinsic information λ^b are fed back to the demodulator, which update the prior symbol probabilities λ^s. After a fixed number of iterations, decisions are made at the output of the channel decoder to generate the decoded bits $\hat{\mathbf{b}}$.

3. Proposed Low-complexity Noncoherent Iterative CPM Demodulator for FH Communication

As we have mentioned, the noncoherent iterative demodulator operates hop-wise. Therefore, without loss of generality, we drop the subscript k for simplification in the following. Notice that $a_{-L+1},\cdots,a_{-1}$ are the last $L-1$ symbols of the previous hop. Here, we use the temporary hard decisions of $a_{-L+1},\cdots,a_{-1}$ as the their values. Without loss of generality, we assume that $a_{-L+1}=\cdots=a_{-1}=1$ and hide the condition $a_{-L+1}=\cdots=a_{-1}=1$ for simplification. Consequently, (4) turns out to be

$$r(t)=s(t;\mathbf{a},\varphi_0)\exp(j\theta)+w(t) \tag{5}$$

Here, we introduce some notations that we will use throughout this paper. We restrict our attentions to the case where M is a power of two, and define $m=\log_2 M$ as the number of bits in each CPM symbol. Denote the input vector for the CPM modulator by $\mathbf{a}=\{a_0,\cdots,a_{N-1}\}$. For each $i=0,\cdots,N-1$, $a_i\in\{\pm1,\pm3,\cdots,\pm M-1\}$ represents an input CPM symbol encoding m bits. The bits encoded in a_i are denoted by $\{a_i^j, j=1,\cdots,m\}$.

For each bit a_i^j, $0\le i\le N-1$, $1\le j\le m$, let $\lambda_{i,j}^b(w)=\Pr(a_i^j=w), w=0,1$ denote the input bit-wise priors provided by the channel decoder. We assume that these bit-wise priors associated with the same block are independent due to the presence of channel interleaver. Based on this independency assumption, the demodulator takes the following three steps to compute the output bit-wise extrinsic information to be passed back to the channel decoder.

1) For each symbol a_i, the demodulator generates symbol-wise priors $\lambda_i^s(a_i)$ from input bit-wise priors $\lambda_{i,j}^b(a_i^j)$ as

$$\lambda_i^s(a_i)=\prod_{j=1}^{m}\lambda_{i,j}^b(a_i^j). \tag{6}$$

2) For each symbol a_i, the demodulator computes symbol-wise APPs $\zeta_i^s(u)=\Pr(a_i=u)$, $u=\pm1,\pm3,\cdots,\pm M-1$ as

$$\begin{aligned}\zeta_i^s(u)&=\Pr[a_i=u\,|\,r(t)]\\ &=\sum_{\varphi_0\in\Phi}\sum_{\mathbf{a}:a_i=u}\Pr[s(t;\mathbf{a},\varphi_0)\,|\,r(t)]\\ &\propto\sum_{\varphi_0\in\Phi}\sum_{\mathbf{a}:a_i=u}\Pr[r(t)\,|\,s(t;\mathbf{a},\varphi_0)]\Pr(\mathbf{a})\Pr(\varphi_0)\\ &=\sum_{\varphi_0\in\Phi}\sum_{\mathbf{a}:a_i=u}\Pr[r(t)\,|\,s(t;\mathbf{a},\varphi_0)]\prod_{i=1}^{N}\lambda_i^s(a_i)\Pr(\varphi_0)\end{aligned} \tag{7}$$

where $\Phi=\{2\pi/P,4\pi/P,\cdots,2\pi(P-1)/P\}$.

Moreover, the temporary hard decisions of $a_i, i=N-L+1,\cdots,N-1$, to be used in the demodulation of the next hop, are obtained by $a_i=\arg\max_u[\zeta_i^s(u)]$.

3) For each bit a_i^j, the demodulator generates updated bit-wise APPs $\zeta_{i,j}^b(w), w=0,1$ and bit-wise extrinsic information $\zeta_{i,j}^{b,e}(w), w=0,1$. The latter is then passed back to the channel decoder.

Using the symbol-wise APPs, we have

$$\zeta_{i,j}^b(w)=\sum_{a_i:a_i^j=w}\zeta_i^s(a_i),\ \ w=0,1. \tag{8}$$

Then the bit wise extrinsic information $\zeta_{i,j}^{b,e}(w)$ is obtained by removing bit-wise priors $\lambda_{i,j}^b(w)$ from $\zeta_{i,j}^b(w)$, i.e.,

$$\zeta_{i,j}^{b,e}(w)=\frac{\frac{\zeta_{i,j}^b(w)}{\lambda_{i,j}^b(w)}}{\frac{\zeta_{i,j}^b(w)}{\lambda_{i,j}^b(w)}+\frac{\zeta_{i,j}^b(1-w)}{\lambda_{i,j}^b(1-w)}}. \tag{9}$$

3.1 Optimal Noncoherent Iterative CPM Demodulator for FH Communication

From (6)-(9), it can be seen that computing $\Pr[r(t)\,|\,s(t;\mathbf{a},\varphi_0)]$ turns out to be the bottleneck in terms of computational efficiency. For optimal noncoherent demodulation, $\Pr[r(t)\,|\,s(t;\mathbf{a}\,,\varphi_0)]$ is described as [2]

$$\Pr[r(t)\,|\,s(t;\mathbf{a}\,,\varphi_0)]\propto I_0\left[\frac{2\left|\int_0^{NT_s}r^*(t)s(t;\mathbf{a},\varphi_0)dt\right|}{N_0}\right] \tag{10}$$

where $I_0(\bullet)$ represents the modified zero order Bessel function of the first kind.

As is seen, the number of the terms in the summation of (7) is equal to M^N, which increases exponentially with the hop length. In contrast to the coherent setting where θ is known, the noncoherent conditional density $\Pr[r(t)\,|\,s(t;\mathbf{a}\,,\varphi_0)]$ shown in (10) cannot be computed recursively, because it does not decompose into a product of suitable individual terms. Therefore, when (10) is used to compute symbol APPs, the resulting complexity is prohibitive, even for moderate hop length.

3.2 Proposed Low-complexity Demodulator Based on Phase Quantization

In this subsection, we introduce a phase quantization approach, which was previously used in the noncoherent demodulation of quadrature amplitude modulation (QAM) in [7], into the demodulation of CPM signals. The main idea of this approach is to approximate the noncoherent channel by a set of coherent channels. It is achieved by discretizing the unknown channel with the phase shift θ.

First, we assume that θ takes only K discrete values in the interval $[0,2\pi)$, i.e.,

$$\theta \in \{0, \frac{1}{K}2\pi, \cdots, \frac{K-1}{K}2\pi\}. \tag{11}$$

Next, we approximate $\Pr[r(t)\,|s(t;\mathbf{a}\,,\varphi_0)]$ as

$$\begin{aligned}
&\Pr[r(t)\,|s(t;\mathbf{a},\varphi_0)\,] \approx \sum_{k=0}^{K-1}\Pr[\theta = 2\pi k/K, r(t)\,|s(t;\mathbf{a},\varphi_0\,)]\\
&=\sum_{k=0}^{K-1}\Pr[\theta=2\pi k/K|s(t;\mathbf{a},\varphi_0)]\Pr[r(t)\,|s(t;\mathbf{a},\varphi_0),\theta=2\pi k/K]\\
&\propto \sum_{k=0}^{K-1}\prod_{i=1}^{N}\exp\{\frac{2\mathrm{Re}[\int_{(i-1)T_s}^{iT_s} r^*(t)s(t;\mathbf{a},\varphi_0)\mathrm{e}^{-j2\pi k/K}dt]}{N_0}\}.
\end{aligned} \tag{12}$$

Finally, we substitute (12) into (7) to approximate $\Pr[r(t)\,|s(t;\mathbf{a},\varphi_0)\,]$ and get the result shown in (13) at the top of the page.

Based on (13), we can compute $\zeta_i^s(u)$ recursively using the BCJR algorithm [12]. The overall computation requirement is equivalent to K times the complexity of a BCJR algorithm applied to the coherent demodulation.

3.3 Complexity Reduction by Exploiting the Phase Rotational Invariance Property of CPM Signals

In this subsection, further complexity reduction is achieved by exploiting the phase rotational invariance property of CPM signals for the proposed demodulator. This approach involves following three steps.

1) It has been known that CPM is rotational invariant to $P-1$ phase ambiguities including $\{2\pi/P, 4\pi/P, \cdots, 2\pi(P-1)/P\}$ [8], i.e.,

$$s(t;\mathbf{a},\varphi_0)e^{j2\pi v/P}\,|_{\varphi_0=\phi} = s(t;\mathbf{a},\varphi_0)\,|_{\varphi_0=\phi+2\pi v/P} \tag{14}$$

where $\phi \in \{0, 2\pi/P, \cdots, 2\pi(P-1)/P\}$ and $v = 0,1,\cdots,(P-1)$.

2) According to (1)-(3), $s(t;\mathbf{a},\varphi_0)$ can be described as

$$s(t;\mathbf{a},\varphi_0) = \Gamma(t;\mathbf{a})\exp(j\varphi_0) \tag{15}$$

where $\Gamma(t;\mathbf{a}) = s(t;\mathbf{a},\varphi_0)\exp(-j\varphi_0)$ is a function unrelated to φ_0. Substituting (10) and (15) into (7), we have

$$\zeta_i^s(u) \propto \sum_{\mathbf{a}:a_i=u} I_0[\frac{2\left|\int_0^{NT_s} r^*(t)\Gamma(t;\mathbf{a})dt\right|}{N_0}]\prod_{i=1}^{N}\lambda_i^s(a_i). \tag{16}$$

According to (16), the output APPs do not depend on the value of φ_0 for noncoherent demodulation. Therefore, without loss of generality, we assume that φ_0 takes any value in $\{0, 2\pi/P, \cdots, 2\pi(P-1)/P\}$ with equal probability. As a result, we have

$$\Pr(\varphi_0 = 0) = \cdots = \Pr(\varphi_0 = 2\pi(P-1)/P) = 1/P. \tag{17}$$

3) We show that, when the quantization level K is an integer multiple of P, (13) can be simplified. Instead of quantizing the phase shift θ in the interval $[0,2\pi)$, we quantize it in the subinterval $[0,2\pi/P)$, thus reducing the number of quantization levels. The reduced phase quantization level K' is equal to K/P. Writing any number k, $0 \le k < K$ in the form $k = p'K' + k'$, where $0 \le p' < P$ and $0 \le k' < K'$, we rewrite (13) as (18), as shown at the bottom of the page.

Define $\Phi(p') = \{2\pi p'/P, 2\pi(1+p')/P, \cdots, 2\pi(P-1+p')/P\}, p' = 0,1,\cdots P-1$. Substituting (14) and (17) into (18), we obtain the result shown in (19) at the bottom of the page.

Finally, using the fact that $s(t;\mathbf{a},\varphi_0)\,|_{\varphi_0=\phi} = s(t;\mathbf{a},\varphi_0)\,|_{\varphi_0=\phi+2\pi}$, $\phi \in \{0, 2\pi/P, \cdots, 2\pi(P-1)/P\}$, we obtain the result shown in (20) at the bottom of the page.

$$\zeta_i^s(u) \propto \sum_{k=0}^{K-1}\sum_{\varphi_0\in\Phi}\sum_{\mathbf{a}:a_i=u}\prod_{i=1}^{N}\exp\{\frac{2\mathrm{Re}[\int_{(i-1)T_s}^{iT_s} r^*(t)s(t;\mathbf{a},\varphi_0)\mathrm{e}^{-j2\pi k/K}dt]}{N_0}\}\lambda_i^s(a_i)\Pr(\varphi_0) \tag{13}$$

$$\zeta_i^s(u) \propto \sum_{k'=0}^{K'-1}\sum_{p'=0}^{P-1}\sum_{\varphi_0\in\Phi}\sum_{\mathbf{a}:a_i=u}\prod_{i=1}^{N}\exp\{\frac{2\mathrm{Re}[\int_{(i-1)T_s}^{iT_s} r^*(t)s(t;\mathbf{a},\varphi_0)\mathrm{e}^{-j2\pi(p'+(k'/K'))/P}dt]}{N_0}\}\lambda_i^s(a_i)\Pr(\varphi_0) \tag{18}$$

$$\zeta_i^s(u) \propto \frac{1}{P}\sum_{k'=0}^{K'-1}\sum_{p'=0}^{P-1}\sum_{\varphi_0\in\Phi(p')}\sum_{\mathbf{a}:a_i=u}\prod_{i=1}^{N}\exp\{\frac{2\mathrm{Re}[\int_{(i-1)T_s}^{iT_s} r^*(t)s(t;\mathbf{a},\varphi_0)\mathrm{e}^{-j2\pi k'/K}dt]}{N_0}\}\lambda_i^s(a_i) \tag{19}$$

$$\zeta_i^s(u) \propto \sum_{k'=0}^{K'-1}\sum_{\varphi_0\in\Phi}\sum_{\mathbf{a}:a_i=u}\prod_{i=1}^{N}\exp\{\frac{2\mathrm{Re}[\int_{(i-1)T_s}^{iT_s} r^*(t)s(t;\mathbf{a},\varphi_0)\mathrm{e}^{-j2\pi k'/K}dt]}{N_0}\}\lambda_i^s(a_i) \tag{20}$$

$$\max_{\mathbf{a}} \Pr(r(t) \left| s(t;\mathbf{a},\varphi_0), \theta = 2\pi k'/K \right.) = \max_{\mathbf{a}} \sum_{\varphi_0 \in \Phi} \prod_{i=1}^{N} \exp\{ \frac{2\mathrm{Re}[\int_{(i-1)T_s}^{iT_s} r^*(t) s(t;\mathbf{a},\varphi_0) \mathrm{e}^{-j2\pi k'/K} dt]}{N_0} \} \lambda_i^s(a_i),\ k' = 0,1,\cdots,K' \quad (21)$$

Demodulator	Additions	Multiplications	Comparisons	Nonlinear functions
PQ demodulator, without phase branch pruning	$4K'NS$	$16K'NS$	0	$4K'N$
PQ demodulator, with phase branch pruning	$4K'N+$ $4GN(S-1)$	$16K'N+$ $16GN(S-1)$	$2N$	$4K'N$
MSDD demodulator	$2^W NS+$ $(4W-2)2^W N$	$W2^W NS+$ $(4W+1)2^W N$	0	$2^W N$
ITS demodulator	$7BNS$	$9BNS$	BNS	$3BNS$
N, S, K', G, W, B denote the hop length, the number of iterations, the number of phase quantization levels for the PQ demodulator, the number of phase quantization levels after first iteration for the PQ demodulator with phase branch pruning, window size for the MSDD demodulator, the number of surviving paths limited by M-algorithm for the ITS demodulator, respectively.				

Tab. 1. Approximated computational complexity per hop for the proposed PQ demodulator, the MSDD demodulator and the ITS demodulator with MSK.

From (14) – (20), it is seen that, by exploiting the phase rotational invariance property of CPM signals, the overall computation requirement is further reduced to K' times the complexity of a BCJR algorithm applied to the coherent demodulation.

3.4 Complexity Reduction by Pruning the Phase Branch

The proposed demodulator implemented using coherent demodulation over K' phase bins incurs a K'-fold complexity increase relative to coherent systems. Numerical results show, however, that a genie-based system, which uses only the phase bins which are closest to the true channel phase, yield comparable performance to K'-fold averaging. We thus investigate a reduced-complexity implementation, which prunes the number of phase branches, especially in later iterations when we have the soft information from the channel decoder. For this purpose, a generalized likelihood ratio test (GLRT) approach, which has been proposed previously in [7], is applied to estimate the phase bins which are closest to the true channel phase.

GLRT operates with the joint probability density function $\Pr(r(t) \left| s(t;\mathbf{a},\varphi_0) \right., \theta)$, and involves following two steps.

1) After first iteration, we maximize the joint likelihood function over the transmitted symbol sequence $\mathbf{a}$ on all K' phase bins, respectively, as shown in (21) at the top of the page.

From (21), it is seen that this step can be viewed as the maximum likelihood sequence estimation (MLSE) and thus can be computed with Viterbi algorithm.

2) G phase bins which maximize the function $\max_{\mathbf{a}} \Pr(r(t) \left| s(t;\mathbf{a},\varphi_0) \right., \theta = 2\pi k'/K)$ are regarded as the phase bins closest to the true channel phase, where G is a design parameter and $0 < G < K'$.

Consequently, after the first iteration, BCJR are computed only on G phase bins instead of K' phase bins with the aid of GLRT. Though this approach will result in performance degradation, it offers a good trade-off between the complexity and performance by varying the value of G.

4. Computational Complexity Analysis

For simplification, in what follows, the proposed demodulator, the demodulator presented in [2], and the demodulator presented in [4], [5] are called PQ (phase quantization) demodulator, MSDD demodulator and ITS demodulator, respectively.

In Tab. 1, the computational complexity analysis for the proposed PQ demodulator with minimum shift keying (MSK) is presented, along with those of the MSDD demodulator and the ITS demodulator. As described in the table, S, W, and B denote the number of iterations, the window size for the MSDD demodulator, and the number of surviving paths limited by M-algorithm for the ITS demodulator, respectively. From the figure, it is seen that the complexity of the MSDD demodulator is exponential to the window size, while the complexity of the proposed PQ demodulator and the ITS demodulator grows linearly with the hop length.

In order to perform a fair comparison between the demodulators, two cases are considered in which the complexity of the demodulators is at the same level, i.e.,

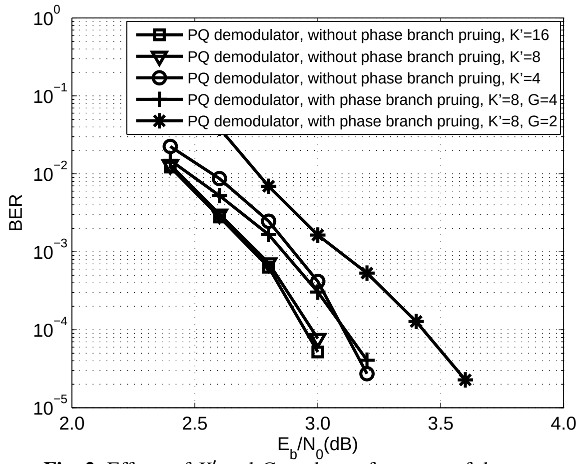

Fig. 2. Effects of K' and G on the performance of the proposed PQ demodulator.

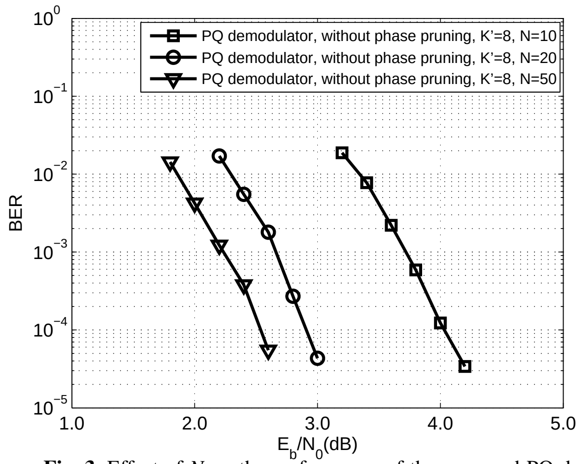

Fig. 3. Effect of N on the performance of the proposed PQ demodulator.

Case 1: $K' = 8$ for the PQ demodulator without phase branch pruning, $W = 4$ for the MSDD demodulator, and $B = 12$ for the ITS demodulator.

Case 2: $K' = 8$, $G = 2$ for the PQ demodulator with phase branch pruning, and $B = 4$ for the ITS demodulator.

Furthermore, as shown in Section 5, the proposed demodulator outperforms the other demodulators in both two cases.

5. Numerical Results

In this section, we give the numerical results by Monte Carlo simulations. Here, the performance of the proposed PQ demodulator is investigated in terms of bit error rate (BER) by simulating the system shown in Fig. 1. Moreover, as described in Subsection 2.2, the simulation channel is modeled as the AWGN channel where the phase offset is assumed to remain constant over each hop and independent from one hop to the next. As in [2] and [4], MSK is considered, and rate 1/2 non-recursive convolutional code with generator polynomial [7 5] is used as the channel code. The length of uncoded bit sequence **b** is set to be 500, the maximum number of iterations is restricted to 7, and BJCR algorithm [12] is used to decode the convolutional code. The hop length N is set to be 20 to provide a good tradeoff between bandwidth-efficiency and power-efficiency of waveforms [2], unless stated otherwise.

Figs. 2 and 3 investigate the effects of the parameters K', G and N on the performance of the proposed PQ demodulator. From the figures, it is seen that

- As expected, the performance of the proposed PQ demodulator improves as the number of quantization levels K' increases. However, increasing K' beyond 8 does not lead to significant performance improvement.
- As G is 4 and 2, the loss in performance due to phase branch pruning at the BER of 10^{-4} is approximately 0.15 dB and 0.45 dB, respectively.
- The performance of the proposed PQ demodulator is an increasing function of the hop length N. This result can be explained as follows. According to (20), the probability for each symbol is evaluated over N symbols in a hop for the proposed PQ demodulator. Therefore, inherently, as N increases, the performance of the proposed PQ demodulator also improves.

As we have mentioned, the complexity of the optimal noncoherent demodulator is prohibitive even for moderate hop length. Therefore, instead of evaluating the performance of the proposed PQ demodulator by the performance of the optimal noncoherent demodulator, we evaluate it by information-theoretic bounds and the performance of the MSDD demodulator. In Fig. 4, the performance of the proposed PQ demodulator and corresponding information-theoretic bound [13] are presented, along with the performance of coherent demodulator [14] assuming perfect phase offset estimation, the information-theoretic bound of coherent demodulation [15], and the performance of the MSDD demodulator with $W = 10$. From the figure, it is seen that

- As $N = 20$, the information-theoretic bound of noncoherent demodulation is approximately 0.75 dB from the information-theoretic bound of coherent demodulation. Moreover, for the proposed PQ demodulator, the loss in performance compared to coherent demodulator at the BER of 10^{-4} is approximately 0.85 dB. This indicates that the performance loss compared to the optimal noncoherent demodulator at the BER of 10^{-4} is approximately 0.1 dB for the proposed PQ demodulator.
- As $K' = 8, W = 10$, the performances of the proposed PQ demodulator and the MSDD demodulator are comparable. Moreover, increasing W beyond 10 only leads

to slightly performance improvement [3]. Therefore, we infer that the performance of the proposed PQ demodulator approaches the performance of the optimal noncoherent demodulator.

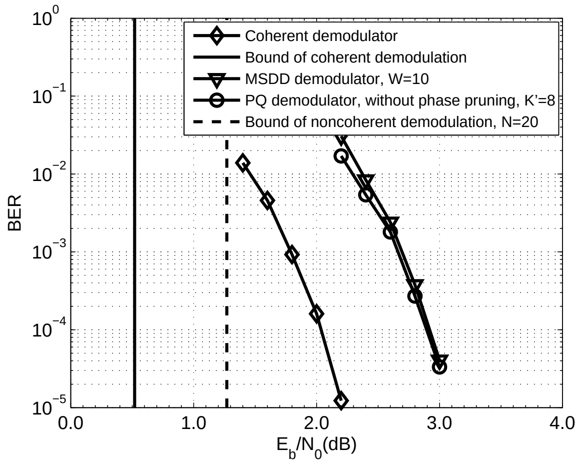

Fig. 4. Performances of the proposed PQ demodulator, coherent demodulator, the MSDD demodulator with $W = 10$, and corresponding information-theoretic bounds.

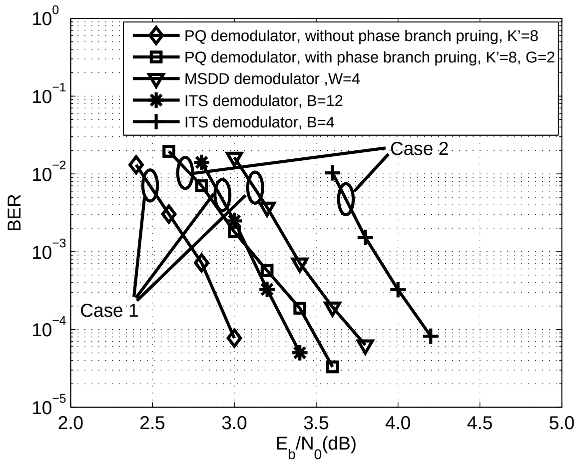

Fig. 5. Performance comparison between the proposed PQ demodulator, the MSDD demodulator, and the ITS demodulator.

Fig. 5 compares the performance of the proposed PQ demodulator and the other demodulators in the two cases mentioned in Section 4. From the figure, it is seen that

- The performance of the proposed PQ demodulator is better than the MSDD demodulator in Case 1. The performance gain is about 0.7 dB at the BER of 10^{-4}.
- The proposed PQ demodulator outperforms the ITS demodulator in both two cases. In Case 1 the performance gain of proposed PQ demodulator compared to the ITS demodulator is about 0.35 dB at the BER of 10^{-4}, while in Case 2 the performance gain is about 0.7 dB at the BER of 10^{-4}.

For the proposed PQ demodulator, the performance improvement over the other demodulators can be explained as follows, i.e.:

- As we have shown, the performance of the proposed PQ demodulator approaches the performance of the optimal noncoherent demodulator.
- For the MSDD demodulator, the probability for each symbol is evaluated over the observation window instead of being evaluated over the hop duration. Consequently, the performance of the demodulator suffers significant losses as window size is much smaller than the hop length.
- The performance of the ITS demodulator suffers significant losses due to two reasons, i.e., the demodulator only exploits part of the symbols over the hop duration to estimate the probability for each symbol and the correct path through the tree may be discarded by M-algorithm.

6. Conclusion

In this paper, a low-complexity noncoherent iterative CPM demodulator for FH communication has been proposed. The effectiveness of the proposed demodulator has been verified with comparisons in terms of the computational complexity analysis and BER simulations. It is clearly shown that the performance of the proposed demodulator approaches the performance of the optimal noncoherent demodulator, and is better than the existing solutions when their complexity is at the same level. Moreover, it is shown that the proposed demodulator also offers a good trade-off between the complexity and performance. Therefore, the proposed demodulator provides an important component for FH-CPM system. Furthermore, though the proposed PQ demodulator is proposed for FH system, it can be also used in many other systems where the phase offset can be assumed to remain constant over a block of symbols, e.g., timing division multiple access (TDMA) system, block-interleaved system, etc.

Acknowledgements

The authors would like to thank the reviewers whose comments led to improvements to the paper.

References

[1] AULIN, T., SUNDBERG, C. E. Continuous phase modulation – parts I and II. *IEEE Transactions on Communication*, 1981, vol. 29, no. 3, p. 196-225.

[2] KIM, H., ZHAO, Q., STUBER, G. L., NARAYANAN, K. R. Antijamming performance of slow FH-CPM signals with concatenated coding and jamming estimation. In *IEEE Military Communications Conference (MILCOM)*. Boston (MA, USA), 2003, vol. 2, p. 1120 - 1125.

[3] NARAYANAN, K. R., STUBER, G. L. Performance of trellis-coded CPM with iterative demodulation and decoding. *IEEE Transactions on Communications*, 2001, vol. 49, no. 4, p. 676 - 687.

[4] BROWN, C., VIGNERON, P. J. A reduced complexity iterative noncoherent CPM detector for frequency hopped wireless military communication systems. In *IEEE Military Communications Conference (MILCOM)*. Atlantic City (NJ, USA), 2005, vol. 4, p. 2345 - 2349.

[5] WANG, G., LI, Q., LI, S. Partial-band jamming suppression with a noncoherent CPM detector. In *International Conference on Communications and Mobile Computing*. Kunming (China), 2009, p. 204 - 208.

[6] FRANZ, V., ANDERSON, J. B. Concatenated decoding with a reduced search BCJR algorithm. *IEEE Journal on Selected Areas in Communications*, 1998., vol. 16, no. 2, p. 186 - 195.

[7] JACOBSEN, N., MADHOW, U. Coded noncoherent communication with amplitude/phase modulation: from Shannon theory to practical architectures. *IEEE Transactions on Communications*, Dec. 2008, vol. 56, no. 12, p. 2040 - 2049.

[8] ZHAO, Q., KIM, H., STUBER, G. L. Innovations-based MAP estimation with application to phase synchronization for serially concatenated CPM. *IEEE Transactions on Wireless Communications*, 2006, vol. 5, no. 5, p. 1033 - 1043.

[9] RIMOLDI, B. A decomposition approach to CPM. *IEEE Transactions on Information Theory*, 1988, vol. 34, no. 2, p. 260 - 270.

[10] BENEDETTO, S., DIVSALAR, D., MONTORSI, G., POLLARA, F. A soft-input soft-output APP module for iterative decoding of concatenated codes. *IEEE Communications Letters*, 1997, vol. 1, no. 1, p. 22 - 24.

[11] BENEDETTO, S., DIVSALAR, D., MONTORSI, G., POLLARA, F. Serial concatenation of interleaved codes: Performance analysis, design and iterative decoding. *IEEE Transactions on Information Theory*, 1998, vol. 44, no. 3, p. 909 - 926.

[12] BAHL, L. R., COCKE, J., JELINEK, F., RAVIV, J. Optimal decoding of linear codes for minimizing symbol error rate. *IEEE Transactions on Information Theory*, 1974, vol. 20, no. 2, p. 284 - 287.

[13] VALENTI, M., CHENG, S., TORRIERI, D. Iterative multisymbol noncoherent reception of coded CPFSK. *IEEE Transactions on Communications*, 2010, vol. 58, no. 7, p. 2046 - 2054.

[14] GERTSMAN, M., LODGE, J. Symbol-by-symbol map demodulation of CPM and PSK signals on Rayleigh flat-fading channels. *IEEE Transactions on Communications*, 1997, vol. 47, no. 7, p. 788 - 799.

[15] CHENG, S., VALENTI, M. C., TORRIERI, D. Coherent continuous-phase frequency-shift keying: parameter optimization and code design. *IEEE Transactions on Wireless Communications*, 2009, vol. 8, no. 4, p. 1792 - 1802.

About Authors...

Yonggang WANG was born in Anhui, China, on January 26, 1985. He received his B.S. degree in communication engineering in 2007 from the PLA University of Science and Technology (PLAUST), Nanjing China. He is currently working toward the Ph.D. degree in satellite communication in PLAUST. His research interests include satellite communication, and digital signal processing.

Aijun LIU was born in 1970, received his Ph.D. degree from Institute of Communication Engineering in 1996. He is currently a professor at PLA University of Science and Technology. His primary research work and interests are in the area of wireless communication and signal processing.

Daoxing GUO was born in 1974, received his Ph.D. degree from Institute of Communication Engineering in 2002. He is currently a professor at PLA University of Science and Technology. His research interests manly fall in the area of satellite communication, adaptive transmission and all digital receivers design.

Xian LIU was born in 1981, received his B.S. degree in communication engineering in 2003 from the PLA University of Science and Technology. He is currently working toward the Ph.D. degree in satellite communication in PLAUST. His research interests include satellite communication, and iterative receiver.